ELSEVIER

Materials Science and Engineering A258 (1998) 84–98

MATERIALS SCIENCE & ENGINEERING A

Recent advances in B2 iron aluminide alloys: deformation, fracture and alloy design

C.T. Liu*, E.P. George, P.J. Maziasz, J.H. Schneibel

Metals and Ceramics Division, Oak Ridge National Laboratory, P.O. Box 2008, Oak Ridge, TN 37831-6115, USA

Abstract

This paper reviews the deformation, fracture and alloy design of B2 iron aluminides based on FeAl. Moisture-induced environmental embrittlement is shown to be a leading cause of low tensile ductility and brittle cleavage fracture of Fe-rich FeAl alloys at ambient temperatures. With increasing Al concentration, two other factors, namely intrinsic grain-boundary weakness and quenched-in vacancies become important in limiting the tensile ductility of FeAl alloys. FeAl alloys show a yield-strength anomaly at intermediate temperatures. Recent work indicates that the anomaly is a result of hardening by thermal vacancies at elevated temperatures. The understanding of the deformation and fracture behavior has led to the development of FeAl-base alloys and composites with improved metallurgical and mechanical properties for structural applications. These FeAl-based alloys can be prepared by melting and casting or by powder processing. The unique combination of the excellent oxidation and carburization/sulfidation resistance coupled with relatively low material density and good mechanical properties at room and elevated temperatures has sparked industrial interest in FeAl alloys and composites for a number of applications. © 1998 Elsevier Science S.A. All rights reserved.

Keywords: FeAl alloys; Tensile ductility; Deformation; Fracture; Thermal vacancies

1. Introduction

Iron aluminides based on Fe_3Al and FeAl are of interest for structural applications at elevated temperatures in hostile environments. This is because they generally possess excellent oxidation and corrosion resistance, relatively low density (as compared with Fe and Ni-base alloys), and low material cost. For the past 15 years or so, considerable effort has been devoted to both understanding the brittle fracture and deformation behavior, and the material processing issues and alloy design of iron aluminide alloys with improved mechanical and metallurgical properties for structural applications. The results of these studies have been documented mainly in the proceedings of a number of intermetallic symposia, including MRS Symposia on High-Temperature Ordered Intermetallic Alloys [1], ASM/TMS Symposia on High Temperature Aluminides and Intermetallics [2], TMS Symposia on Structural Intermetallics [3], and Deformation and Fracture of Ordered Intermetallic Materials [4]. Also, iron aluminides were the subject of three recent topical conferences, namely: (1) Processing, Properties and Applications of Iron Aluminides organized by Schneibel and Crimp [5]; (2) Nickel and Iron aluminides: Processing, Properties and Applications organized by Deevi et al. [6]; and (3) Iron Aluminides: Alloy Design, Processing, Properties and Applications organized by Deevi et al. [7]. Readers are urged to refer to these proceedings volumes for detailed information about iron aluminide alloys.

Two keynote papers were presented at the present Symposium on Iron Aluminides: (1) Iron aluminides — present status and future prospects by Stoloff; and (2) Recent advances in B2 iron aluminide alloys: deformation, fracture and alloy design by Liu et al. In the first keynote paper, Stoloff summarizes the cur-

* Corresponding author.

0921-5093/98/$ - see front matter © 1998 Elsevier Science S.A. All rights reserved.
PII S0921-5093(98)00921-6

rent status of our understanding of the mechanical properties, alloy design, and processing of Fe_3Al iron aluminide alloys [8]. This second keynote paper focuses on the recent advances in B2 iron aluminides based on FeAl. For the past decade, a great deal of effort has been devoted to the studies of the mechanical and metallurgical properties of FeAl alloys. Because of page limitations, this review on FeAl alloys is focused only on recent progress on the deformation, fracture and alloy design of FeAl alloys for structural use.

2. Brittle fracture and low tensile ductility

Since the discovery of moisture-induced environmental embrittlement in iron aluminides in 1989 [9], extensive studies have been devoted to the understanding of brittle fracture and low tensile ductilities of iron aluminides [10–16]. Recent studies indicate that there are three major causes of the low tensile ductility and brittle fracture of FeAl aluminides at ambient temperatures: (1) environmental embrittlement; (2) weak grain boundaries; and (3) vacancy hardening and embrittlement. Environmental embrittlement involving moisture in air is a major cause of low tensile ductility of both Fe_3Al and FeAl aluminides [16]. Environmental embrittlement is the only major cause for Fe_3Al alloys, whereas grain boundary weakness and vacancy hardening are two more reasons for low tensile ductilities in FeAl alloys with Al levels above 38 at.% [11,17]. When intergranular fracture becomes a dominant fracture mode for FeAl alloys, their tensile ductility at room temperature also depends on grain size, with better ductilities for small-grained materials [18].

2.1. Environmental embrittlement

Fe_3Al and FeAl alloys were considered to be intrinsically brittle at room temperature because of their poor cleavage strength and difficulty in cross slip in ordered lattices. In 1989, Liu et al. first reported that FeAl alloys containing less than 40% Al are intrinsically quite ductile, and that the low tensile ductility and cleavage fracture were caused mainly by environmental embrittlement involving moisture in air [9]. The environmental effect is vividly demonstrated in Fig. 1. An FeAl alloy (36.5% Al) showed brittle cleavage fracture and only 2.2% tensile elongation when tested in air at room temperature. The same alloy tested in a conventional vacuum had a ductility of about 8%. Ultimately, the alloy exhibited a tensile ductility as high as 18% when tested in a dry oxygen environment. The same embrittlement effect was also observed in single-crystal FeAl alloys [19,20].

Mechanistically, the environmental embrittlement is explained by a chemical reaction involving the interaction of Al atoms with moisture in air and the generation of hydrogen [9,16]. The penetration of atomic hydrogen at the crack tip results in hydrogen-induced embrittlement in iron aluminides and other intermetallic alloys. Systematic studies of the embrittling effect as functions of test temperature, strain rate, and shielding gas have indicated that the severity of the embrittlement depends on two kinetic parameters: the moisture/aluminide reaction kinetics and the hydrogen diffusion rate in aluminides. The embrittlement can be substantially reduced by controlling test environments, increasing strain rates and using shielding gases [16,21–24]. As shown in Fig. 1,

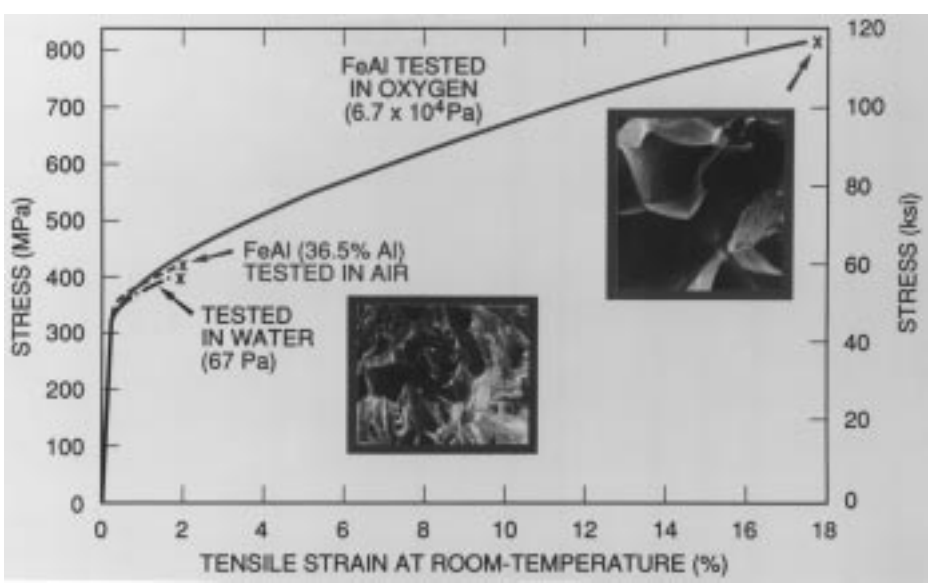

Fig. 1. Stress-strain behavior of Fe-36.5%Al at room temperature in various environments [9].

the room-temperature tensile ductility increased from 2.2% in ambient air to 18% in dry oxygen.

The hydrogen-induced environmental embrittlement affects not only tensile ductility but also cleavage planes [19,20,25,26]. Table 1 summarizes the effect of Al concentration on cleavage fracture planes of iron aluminides tested in different test environments at room temperature. This table shows that FeAl aluminides fractured mainly by {100}-type cleavage when tested in moist air. With increasing Al concentration from 35 to 50%, the cleavage fracture gradually changed from {100} to {110} types in vacuum. These observations suggest that moisture-induced hydrogen promotes {100} cleavage fracture in FeAl alloys with high Al concentrations.

First-principles calculations were used to understand the electron concentration and atomic bonding in FeAl. The calculations by Fu and Painter [27] showed that interstitial hydrogen absorbs electrons from iron atoms and reduces the cleavage strength of {100} planes by as much as 70%. This result is consistent with the observed {100} cleavage when FeAl is tested in moist air. Li and Liu [28] suggest that interstitial hydrogen in FeAl alloys also promotes crack nucleation on {100} planes. As schematically shown in Fig. 2, the Cottrell mechanism is enhanced by reducing the energy of a ⟨010⟩ dislocation in B2 alloys through the segregation of hydrogen atoms to the dislocations. The ⟨111⟩ dislocations stabilized by hydrogen can serve as crack nucleus for the {100} cleavage fracture in FeAl alloys. The ⟨010⟩ dislocations were observed in a FeAl alloy by Munroe and Baker [29].

2.2. Grain-boundary weakness in FeAl alloys

As pointed out earlier, environmental embrittlement is not the only reason for poor ductility and brittle fracture in FeAl alloys. With increasing Al concentration, another factor, namely intrinsic grain-boundary weakness, becomes important in limiting the tensile ductility of FeAl [11].

In order to understand the intrinsic grain-boundary weakness of FeAl alloys, first let us examine the effect of boron addition on tensile properties of FeAl (40% Al). Boron is known to segregate to the grain boundaries of FeAl [10,11] and suppress intergranular fracture [10,11,30,31]. However, as shown in Table 2, the addition of B increases ductility only modestly, from 1.2 to 4.3%. The reason is that the beneficial role of B in FeAl is related mainly to the enhancement of grain-boundary cohesion. But weak boundary cohesion is not the only factor limiting the ductility of FeAl; environmental embrittlement is another major factor. Boron has little effect on suppressing environmental embrittlement, which occurs transgranularly in FeAl. This is unlike in Ni_3Al where it occurs intergranularly and B can therefore suppress it [32,33]. As a result, B is relatively ineffective in improving the ductility of Fe-40Al. Both environmental embrittlement and grain-boundary fracture need to be suppressed, and when that is done (by testing the B-doped alloy in oxygen), high ductilities approaching 17% are obtained (Table 2).

In order to study the 'intrinsic' mechanical behavior of FeAl, Cohron et al. [17] recently tested it in ultra-high vacuum (i.e. in the absence of environmental effects). Their results are summarized in Fig. 3. In

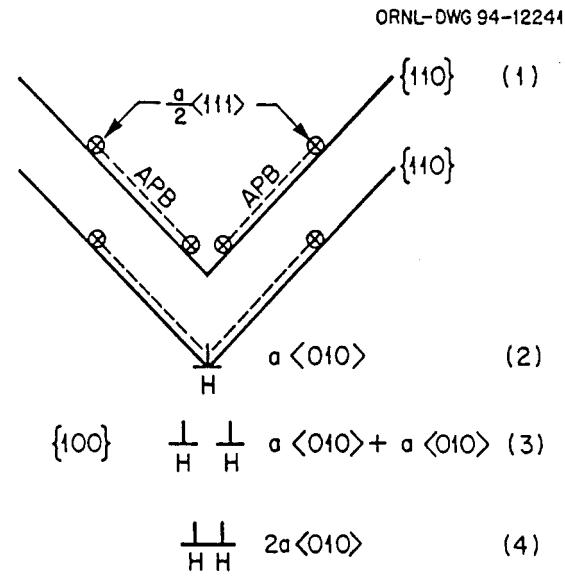

Fig. 2. Cottrell mechanism enhanced by hydrogen segregation to a ⟨010⟩ dislocation [28].

Table 1
Effects of test environment and Al level on cleavage fracture plane in FeAl alloys

Al concentration (at. %)	Cleavage plane		
	Vacuum	Air	References
35	{100} + others	{100} + others	[19]
40	{100} + others	More {100}	[20,25]
50	{111}	{100}	[26]

Table 2
Effect of test environment on the room-temperature tensile properties of B-free and B-doped Fe-40Al [11]

Alloy	Environment	Ductility (%)	Yield strength (MPa)	Fracture mode FeAl
FeAl	Air	1.2	390	GBF
FeAl	Oxygen	3.2	402	GBF
FeAl + B	Air	4.3	391	TF
FeAl + B	Oxygen	16.8	392	TF

GBF, grain-boundary fracture; TF, transgranular fracture.

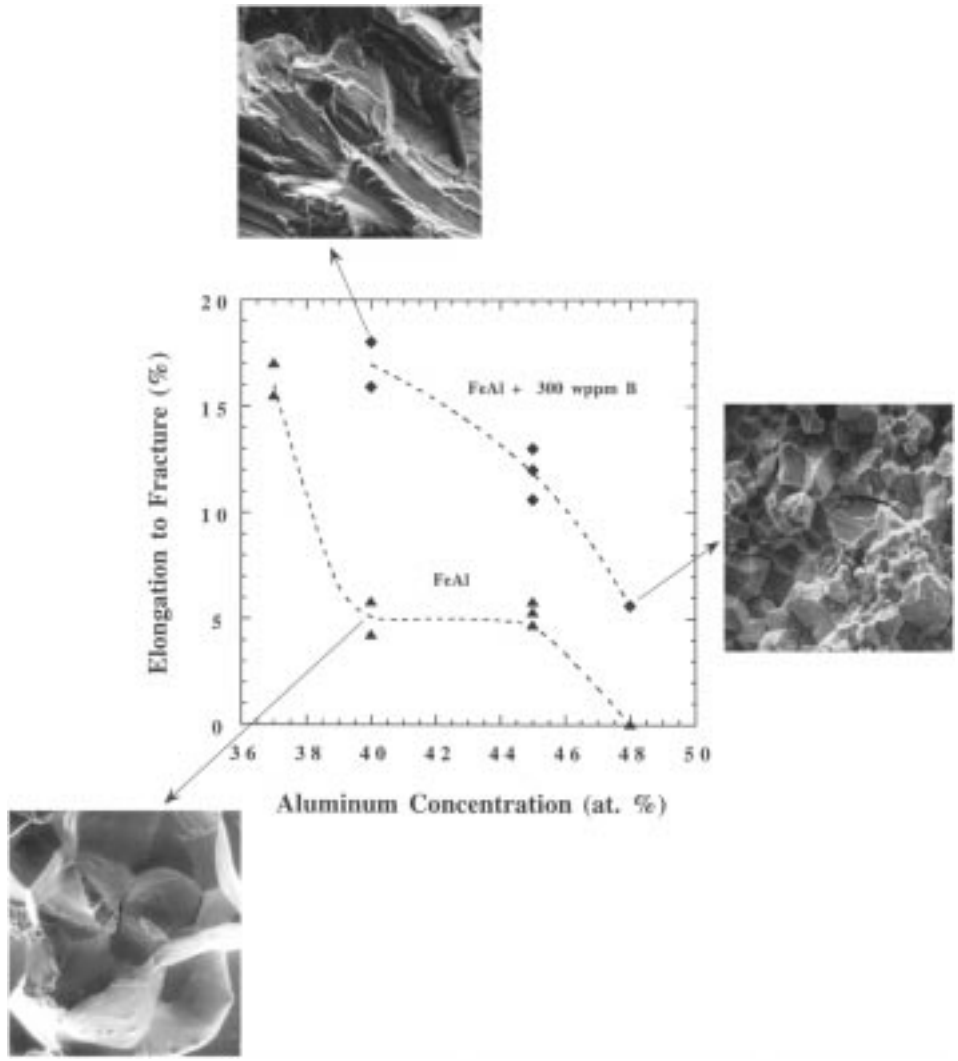

Fig. 3. Tensile ductility and fracture behavior of B-free and B-doped FeAl alloys in ultrahigh vacuum [17].

ultrahigh vacuum, the intrinsic ductility of B-free FeAl drops off precipitously as the Al concentration increases beyond 37%. Additionally, the fracture mode changes from transgranular to intergranular as the ductility decreases. Together, these results confirm our earlier suggestion [11], which was based on tests conducted in oxygen, that the grain boundaries in FeAl become intrinsically brittle as the Al concentration increases.

When B is added to FeAl, intergranular fracture is suppressed and the composition of the ductile-brittle transition is shifted to higher Al levels (Fig. 3). As mentioned earlier, the beneficial effect of B stems from its segregation to the grain boundaries where it presumably enhances grain-boundary cohesion. However, with increasing Al concentration, B is less able to suppress intergranular fracture in FeAl (Fig. 3). A similar behavior was noted also in Ni_3Al [34]. In that case, however, B segregated less strongly to the grain boundaries of Ni_3Al as the Al concentration increased. In FeAl, by contrast, the segregation of B is essentially independent of Al concentration [17]. Apparently, the grain boundaries in near-stoichiometric FeAl become so weak that, even though B segregates strongly, it is unable to strengthen them effectively.

2.3. Vacancy hardening and embrittlement

Thermal vacancies are easy to introduce in FeAl alloys containing $>38\%$ Al by fast cooling from heat treatments at elevated temperatures [35–37]. A detailed discussion of the thermal-vacancy hardening in FeAl alloys will be given in Section 3.

Recently, Yang et al. [38] have demonstrated the embrittling effect of thermal vacancies in FeAl alloys. Table 3 shows the severe embrittlement of FeAl (40% Al) by thermal vacancies introduced by fast cooling. An increase in quenched-in thermal vacancies from 1.3×10^{-2} to 62×10^{-2} reduces the tensile ductility in vacuum from 7.4 to 2.9% at room temperature. A

Table 3
Effect of vacancy concentration on tensile properties of FeAl (40% Al) at room temperature [38]

Vacancy concentration (at.%)	Tensile elongation (%)	Fracture strength (MPa)
Vacuum test		
1.3×10^{-2}	7.4	734
62×10^{-2}	2.9	969
Air test		
1.3×10^{-2}	0.7	420
62×10^{-2}	0.1	714

similar embrittling effect is also observed in air; however, the alloy showed much lower ductility in air because of additional embrittlement imposed by moisture in air. It is interesting to note that the thermal vacancies in the FeAl alloy promote cleavage fracture along {110} slip planes, as reported by Yang et al. [38].

3. Vacancy hardening and yield strength anomaly

In 1956, Westbrook [39] first indicated that the defect hardening behavior was different in B2 alloys. This is shown in Fig. 4, where the yield strength is plotted as a function of Al concentration. NiAl and CoAl alloys showed a minimum hardness at the stoichiometric composition, whereas FeAl alloys exhibited a steady increase in hardness with increasing Al concentration across the stoichiometric composition. This difference in the hardening behaviors was not understood for more than three decades. In 1990 Nagpal and Baker [40] demonstrated that the unusual

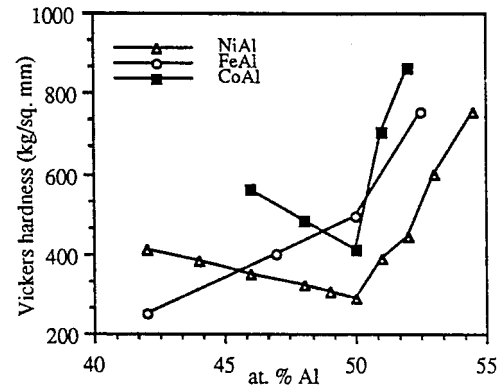

Fig. 4. Vickers hardness of CoAl, FeAl and NiAl as a function of composition [39].

hardening behavior is caused mainly by thermal vacancies that are easily introduced in FeAl alloys with high Al concentrations. Their work stimulated great interest in the study of thermal vacancies in FeAl alloys.

Chang et al. [35] conducted a systematic study of the effect of thermal vacancies on the microhardness of FeAl alloys containing 40–51% Al. The thermal vacancies were introduced by quenching the alloys from different temperatures. Figures 5 and 6 summarize the results of their studies. As shown in Fig. 5, the room-temperature hardness of the alloys increases with both the quenching temperature and Al concentration. In order to correlate the hardness with thermal vacancies, the vacancy concentration was estimated by a triple defect model developed by Neumann and Chang [41,42]. As shown in Fig. 6, the hardness is correlated well with the estimated vacancy

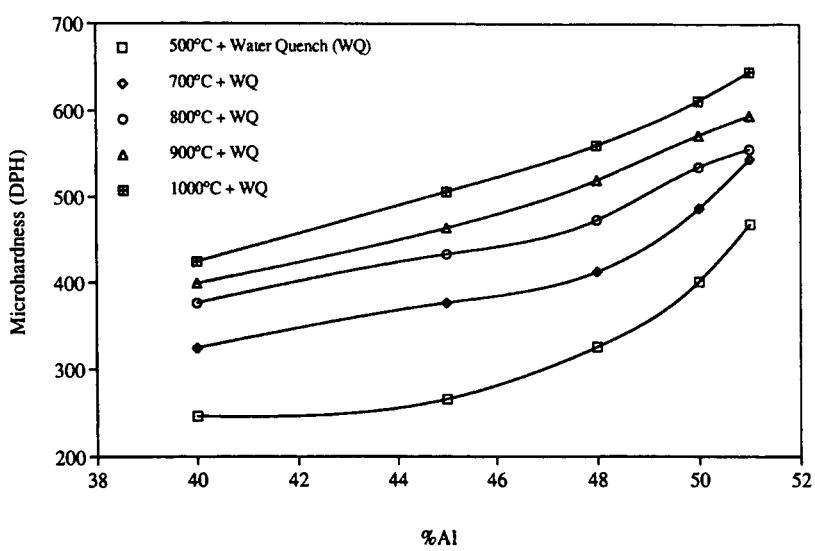

Fig. 5. Room-temperature hardness of FeAl as a function of Al concentration in samples heat treated and quenched from high temperatures [35].

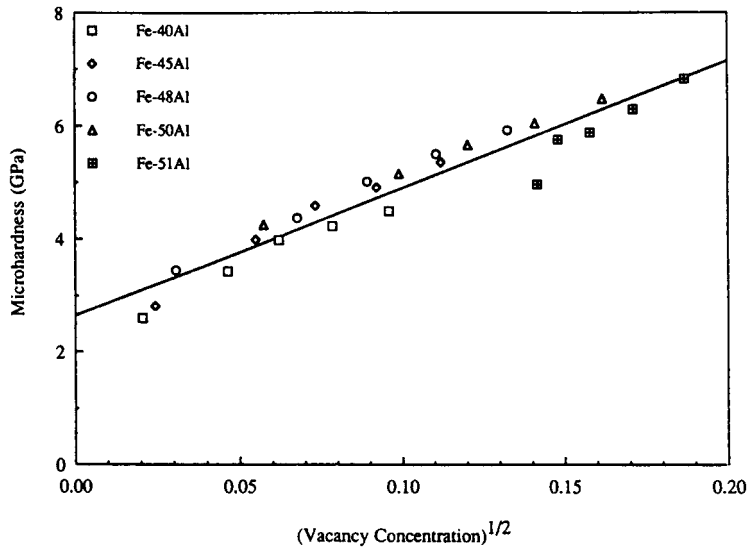

Fig. 6. Relationship between the microhardness and the square root of the vacancy concentration in FeAl alloys [35].

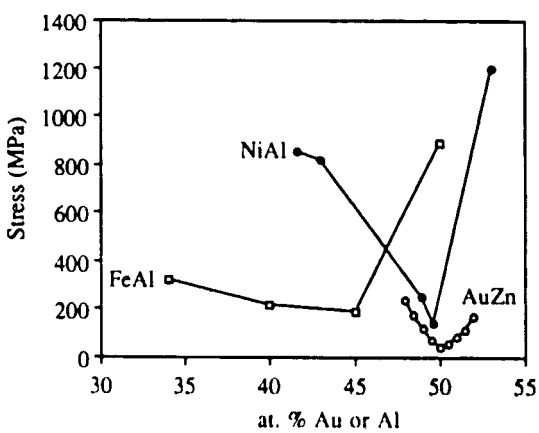

Fig. 7. Yield strength of B2 intermetallics as a function of composition [43].

concentration through the classic solute hardening relationship, that is, the hardness is proportional to (vacancy concentration)$^{1/2}$. This relationship provides strong evidence that the increase in room-temperature hardness in FeAl alloys is due to quenched-in thermal vacancies. By careful reduction of thermal vacancies via low-temperature annealing, Baker [43] demonstrated that the defect hardening behavior of FeAl alloys was not different from other B2 intermetallics (Fig. 7). Note that the hardness minimum for FeAl alloys is located at 45% Al, rather than 50% Al commonly observed for other B2 alloys. This difference can be rationalized from the fact that thermally-induced vacancies in FeAl alloys with more than 45% Al are very difficult to anneal out even after extensive annealing at a low temperature of 400°C [37,44]. The hardening due to retained vacancies in high Al alloys shifts the hardness minimum from 50% to $\approx$ 45% Al in FeAl alloys (Fig. 7).

The yield strength of FeAl, instead of decreasing with temperature, shows an anomalous increase at intermediate temperatures (e.g. [36,45–48]). The yield anomaly tends to be obscured, however, if the specimens are not carefully annealed at low-enough temperatures to eliminate quenched-in thermal vacancies prior to the test [48]. As shown in Fig. 8, specimens annealed at 700°C for 2 h (which contain quenched-in vacancies) exhibit the conventional decrease in strength with increasing temperature followed by a plateau region and a further decrease in strength with increasing temperature. In contrast, specimens given a long-term vacancy-minimizing anneal (5 days at 400°C, bottom curve), clearly show the anomalous increase in strength at intermediate temperatures.

Several early attempts to explain the source of the yield anomaly in FeAl were unsuccessful, as detailed by George and Baker [49,50]. Recently, Carleton et al. [48] suggested that the yield strength anomaly in FeAl may be the result of hardening by thermal vacancies. George and Baker [49] then modeled the temperature dependence of the yield strength of FeAl in terms of solid-solution hardening by thermal vacancies at intermediate temperatures and vacancy-enhanced dislocation creep at elevated temperatures. Their results are shown in Fig. 9, where the circles represent experimental data for Fe-40Al, the solid lines represent best fits of the George–Baker model to the experimental data, and the dotted lines the model's prediction for the change in yield strength (beyond the peak temperature) with increasing strain rate. George and Baker [49] showed that strength increases comparable to those observed in the anomalous region ($\sim$ 80 MPa) are explainable with the vacancy concentrations ($\sim 10^{-4}$, [35]) present at the peak temperature. Also, by fitting their model to the yield strength data, they

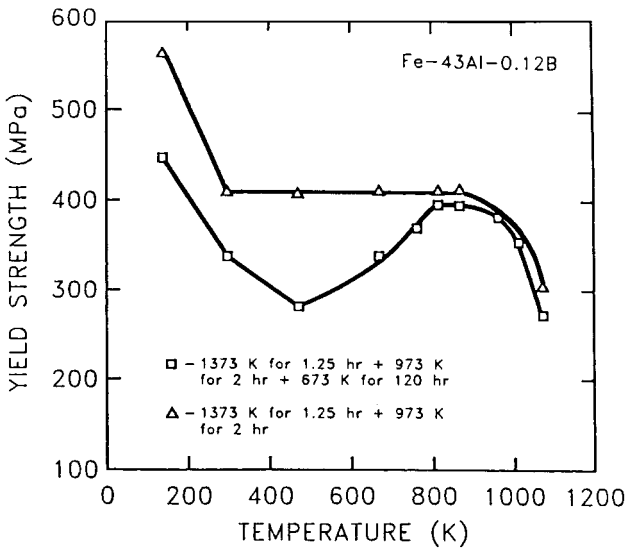

Fig. 8. Effect of heat treatment on the temperature dependence of the yield strength of B-doped Fe-40Al [48]. Only well-annealed samples containing low levels of residual vacancies exhibit the yield anomaly; quenched-in vacancies obscure it.

obtained a value for the vacancy formation energy of 92 kJ/mol. This is remarkably close to the experimental value for this parameter of 95 kJ/mol obtained by positron annihilation [51], a result which strongly supports the model. Similarly, the value of the vacancy migration energy obtained from the George–Baker model also agrees with that measured by Würschum et al. [51].

In the model, yield strength depends on strain rate only above the peak temperature and not below [49]. A consequence of this is that the point of intersection of these two regions shifts to higher (or lower) temperatures as the strain rate increases (or decreases) (Fig. 9). These implications have been confirmed experimentally in B-doped [49] and B-free [52] Fe-40Al: in both, the yield stress in the anomalous region is relatively insensitive to strain rate, but the peak temperature and the peak stress depend on strain rate (because of the strain-rate dependence of Region IV, Fig. 9). In fact, at low-enough strain rates, Region IV shifts so much to the left that the yield anomaly almost completely disappears [52].

George et al. [53] corroborated the vacancy-hardening mechanism by performing experiments in a Gleeble machine in which specimens can be rapidly heated (up-quenched, at 300 K s^{-1}) and cooled (down-quenched, at 100 K s^{-1}). Their procedure consisted of taking well-annealed specimens of Fe-40Al (containing low vacancy concentrations), up-quenching them to the peak temperature (T_p), holding for various lengths of time, and then tensile testing at a strain rate of 2.4×10^{-3} s^{-1}. Their results are shown in Fig. 10. Since the generation of the equilibrium vacancy concentration at T_p is not instantaneous, the yield strength after very short hold times (1 s) was found to be comparable to that at room temperature. With increasing hold time at T_p, however, the yield stress was found to increase progressively. Eventually, at times of 30 min or longer, the yield strength became independent of hold time because the vacancy concentration presumably reached the equilibrium value in about half an hour. The quenching experiments were performed without any tensile loads being imposed on the specimens. Tensile loading occurred only after the quench was completed. The time required to reach 0.2% strain (at which the yield stresses were measured) was ~0.8 s in all cases, which is short compared to the hold times at which a change in the yield strength was noted (30 s, 300 s, and 0.5 h). Clearly, the changes in yield strength at T_p are a result of changes during the stress-free holding pe-

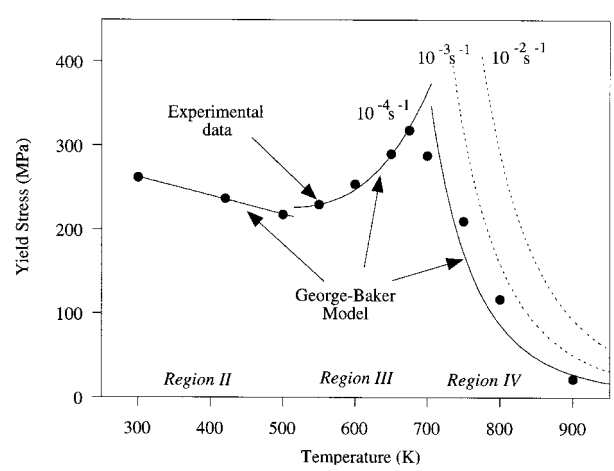

Fig. 9. Temperature dependence of the yield strength of Fe-40Al [49]. The circles represent experimental data, solid lines the George–Baker model, and dotted lines the model's prediction of the strain rate dependence of yield strength.

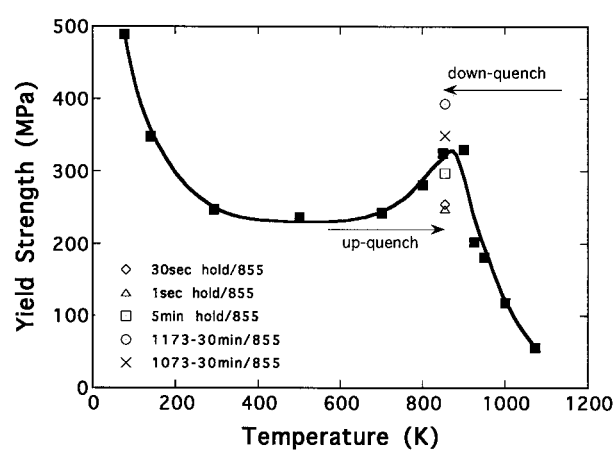

Fig. 10. Yield strengths after various up-quenching and down-quenching heat treatments in the Gleeble machine compared to those measured in an Instron tensile test (solid curve) [53].

riod, rather than during the tensile test. The simplest explanation is that the vacancy concentration increases with increasing hold-time, resulting in an increase in the yield strength. Additionally, the time constant of this increase in yield strength fits perfectly with that for the diffusivity of vacancies obtained in positron annihilation and internal friction measurements [54].

Fig. 10 also shows results of down-quenching experiments in which specimens were equilibrated at high temperatures (1073 or 1173 K), cooled rapidly to T_p, and immediately tensile tested. The yield strengths of these specimens were found to be higher than those of specimens slowly heated to T_p from room temperature, consistent with the higher vacancy concentrations in the down-quenched specimens. As pointed out by George and Baker [50], this 'path dependence' of the yield strength at T_p rules out dislocation-type models for the strength anomaly (e.g. cross-slip pinning, climb dissociation, or glide decomposition) because they would predict the same yield strength regardless of the path taken to arrive at T_p. The vacancy mechanism, in contrast, depends sensitively on thermal history, consistent with the effects shown in Fig. 10.

4. Alloy design of FeAl alloys

The understanding of the deformation and fracture behavior has led to the development of physical metallurgy principles for design of ductile and strong FeAl alloys for structural use. The general principles deduced from this understanding include the following:

1. controlling the Al level $< 38\%$,
2. producing wrought/fibrous/elongated grain structures,
3. refining grain size,
4. forming protective surface coating/layer (e.g. oxide coating),
5. minimizing thermal vacancies by slow cooling from $> 400°C$, and
6. adding beneficial alloying elements, including
   - boron: to strengthen grain boundaries,
   - carbon: to improve weldability and form carbides,
   - Zr borides/carbides: to refine grain size and retain fibrous grain structure, and
   - Mo: to improve strength and creep resistance.

An example of substantial improvement of the ductility of a FeAl alloy is shown in Table 4 [16]. The refinement of grain size by adding 0.05 Zr and 0.24 B increased the room-temperature ductility of FeAl (35.8% Al) from 2.2 to 10.7%. The addition of B also enhanced the grain-boundary cohesion and suppressed intergranular fracture of the alloy. Usually, preoxidation leads to a decrease in the ductility of alloys. However, the formation of protective oxide layers by preoxidation at 700°C alleviated moisture-induced environmental embrittlement and further improved the tensile ductility of the FeAl alloy from 10.7% to 14.2%, i.e. 33% increase in room temperature ductility.

Table 4
Influence of alloy addition and preoxidation on room-temperature (RT) tensile ductility of FeAl alloys [16]

Alloy composition (at.%)	Elongation (%)	Strength (ksi)	
		Yield	Tensile
FeAl (35.8Al)	2.2	51.6	59.4
FeAl + 0.05Zr + 0.24B	10.7	48.2	109.6
FeAl + 0.05Zr + 0.24B + preoxidation[a]	14.2	51.8	134.0

[a] To form protective oxide scales at 700°C.

The B2 FeAl alloys are generally more brittle at room temperature and weaker at higher temperatures than Fe_3Al alloys or iron-aluminides with even less Al [54–56]. Therefore, FeAl alloys have not been as much the subject of alloy development studies, until recently [56–63]. Recently, FeAl alloys have been found to have outstanding high-temperature oxidation and corrosion resistance in various aggressive environments, including resistance to carburization, sulfidation and molten carbonate salt attacks. Such corrosion resistance based on their formation of adherent, compact alumina scales, together with several recent breakthroughs in alloying and/or processing effects on mechanical properties [61–65], is driving a serious alloy development effort on FeAl alloys at Oak Ridge National Laboratory (ORNL), particularly on cast FeAl alloys.

The Fe-(36–40)Al-0.2Mo-0.05Zr-0.13C (at.%) alloys were originally developed as wrought material at ORNL in the early 1990s. The Mo and Zr were added for improved high-temperature strength and room-temperature ductility [59], and C replaced B to prevent hot-cracking and make these FeAl alloys more weldable [67]. Micro-alloying additions of boron (100–200 at. ppm) were found to dramatically improve the weldability, and to improve the room-temperature ductility and resistance to environmental embrittlement (as measured by comparing tensile ductility in air and in oxygen at room-temperature) of wrought and cast I/M FeAl material [65,66]. In cast FeAl alloys, ductility improved from 2 to 4–5% by B modestly refining the grain size and changing the fracture mode from intergranular to transgranular quasi-cleavage [62]. Boron micro-alloying additions were also found to significantly improve the high-tem-

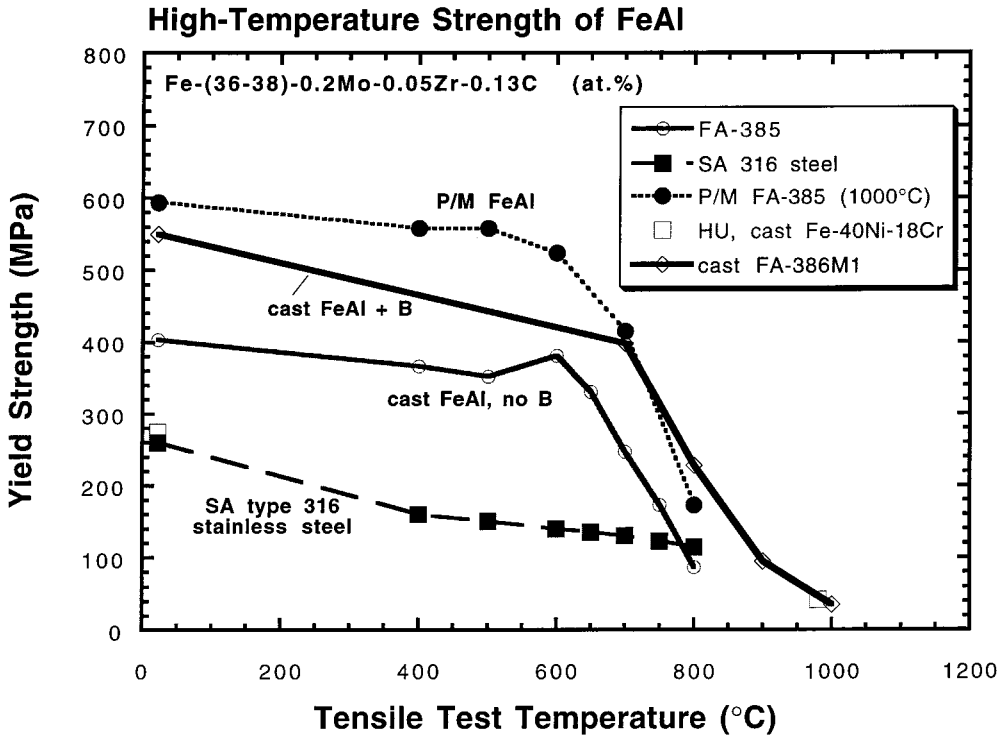

Fig. 11. Yield strength (YS) plotted as a function of temperature for FeAl alloys with the base composition or minor modifications of that composition, in the cast (coarse grained) or hot-extruded P/M (very fine-grained) conditions. The properties of wrought and solution-annealed (SA) type 316 and cast HU austenitic stainless steels and alloys are included for comparison [62].

perature yield strength (Fig. 11) and the creep-resistance of these new FeAl alloys in the cast condition, by promoting enhanced formation and stability of fine ZrC precipitates [62]. These same micro-alloying additions of B were found to dramatically improve the Charpy-impact toughness of hot-extruded, fine-grained FeAl from 25 to 65 J (Fig. 12). The improved toughness also correlated with a change in the fracture mode from intergranular to transgranular quasi-cleavage [65]. Cast FeAl alloys with much coarser grain sizes than the hot-extruded material (100–250 μm or more compared to 35–50 μm) were still found to have Charpy impact energies of about 15 J, and to improve to as high as 30 J with additions of more Zr and C in conjunction with B (Fig. 12) [65]. A second generation of cast FeAl alloys with more Zr and C also shows improved high-temperature yield strength and creep-rupture resistance (Fig. 11) [62].

Probably the most dramatic improvement in room-temperature ductility, toughness and fracture behavior of FeAl alloys was found when P/M FeAl alloys were produced by hot-extrusion at 950, 1000, and 1100°C to directly consolidate the powders [65]. Dramatic improvements in ductility (12–15% in air, 20–30% in oxygen) and strength (yield strength, 600–670 MPa) were found in P/M FeAl with ultra-fine grain-sizes (3–4 μm) produced by hot-extrusion at 950–1000°C to recrystallize the material without

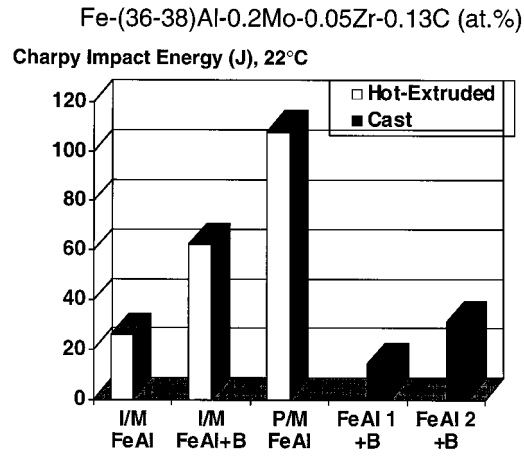

Fig. 12. Charpy energies for tests in air at room-temperature of ingot-metallurgy (I/M) FeAl hot-extruded at 900°C, with and without microalloying additions of boron (35–50 μm grain size), P/M hot-extruded at 950°C (3 μm grain size), and cast FeAl alloys with boron (FeAl1) and other minor alloying additions (FeAl2) (100–250 μm grain size). Clearly, both minor alloying additions and microstructure affect impact energy, and all alloys have more than the 3–5 J impact energy shown for FeAl previously [62,64,65].

much subsequent grain growth (Fig. 13). These ultra-fine grained P/M FeAl alloys exhibited ductile trans-granular dimple fracture instead of the typical trans-granular quasi-cleavage found at slightly larger grain sizes (9 μm) (Fig. 13). These strong and ductile P/M

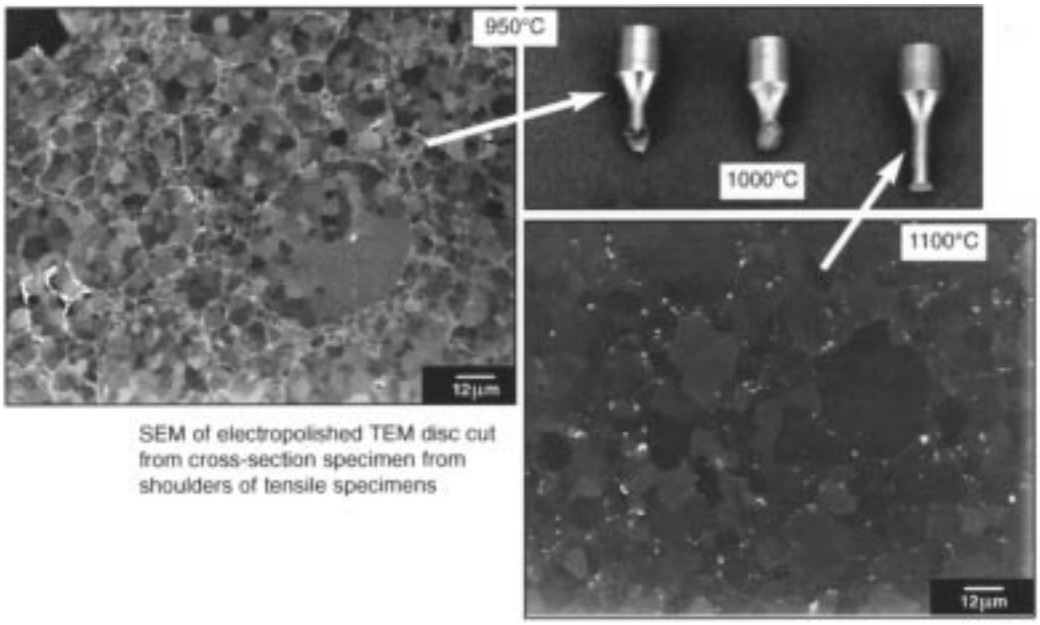

Fig. 13. SEM micrographs of electropolished TEM disks, showing differences in the grain size and remnant oxide structures from deformed powder particles, and portions of tensile specimens fractured in oxygen at room-temperature of P/M FeAl alloys directly consolidated by hot-extrusion at the temperatures indicated. Extrusion at 950 and 1000°C produces similar, very fine grained (3–4 μm diameter) material that fractures in a ductile manner, even in air. Extrusion at 1100°C produces a coarser grain size (9 μm) and more brittle fracture [64].

FeAl alloys also showed the highest Charpy impact toughness values (up to 108 J, Fig. 12) ever found in any FeAl alloy [65]. However, unlike the P/M FeAl tensile specimens, there is a strong influence of the microstructural texture created by the deformation of the powder particles with thin oxide coatings during hot-extrusion. These elliptical particles shear to deflect cracks during impact testing and create the shear-lips observed on the macroscopic fracture surface (Fig. 14). Extrusion at 1100°C in addition to producing coarser grains also removes this remnant particle oxide texture, resulting in more typical planar fracture and lower toughness (Fig. 14).

Alloy development to improve the mechanical properties of FeAl alloys processed by various methods continues. Ductile, finer-grained FeAl alloys with 8–10% or more room-temperature ductility are readily weldable with no evidence of cold-cracking. Cast FeAl alloys exhibit varying degrees of cold-cracking after welding, but an alloy with about 4.5% ductility in air was found not to cold-crack. It appears that the best chances for further overall property improvements in FeAl alloys will come from carefully controlling micro-alloying additions together with the processing-induced microstructure.

5. Material processing and structural applications

FeAl-based alloys, just like Fe_3Al alloys, can be prepared by conventional melting and casting techniques or by powder processing. A number of papers by Sikka, Deevi, and others [63,68–70] have been focused on the processing of iron aluminide alloys. Since iron aluminides readily absorb hydrogen in their molten state and form hydrogen gas bubbles during casting, it is important to remove rust scales from charge materials prior to melting. Also, cover gases, such as He and Ar, are required if iron aluminide alloys are melted in moist air. FeAl alloys can be fabricated by hot forging, rolling or extrusion. Because of their low ductility, FeAl alloys are generally fabricated at about 100–300°C above the temperatures used for Fe_3Al alloys. For instance, cast FeAl alloy ingots containing 35 to 40% Al can be fabricated by hot forging at 1000–1200°C, followed by warm rolling at 800–1000°C. In order to retain the heat during hot working, cladding materials are often used to wrap FeAl alloy for plate and sheet fabrication.

FeAl materials are successfully produced by powder processing, using elemental Al and Fe powders or alloy powders with and without ceramic additives [63,65,69]. Alloy powders can be made in inert gas or water coolant, and then consolidated by hot pressing or hot extrusion. Maziasz et al. [65] found that the microstructures and mechanical properties of FeAl alloys were controlled by hot extrusion of water-cooled alloy powders. Hot extrusion at 950–1000°C resulted in fine grain structures, which showed excellent tensile strength and ductility at room and elevated temperatures. Hot extrusion at 1100°C, on the other hand, produced a coarse grain structure, which exhibited lower tensile ductility and fracture toughness at

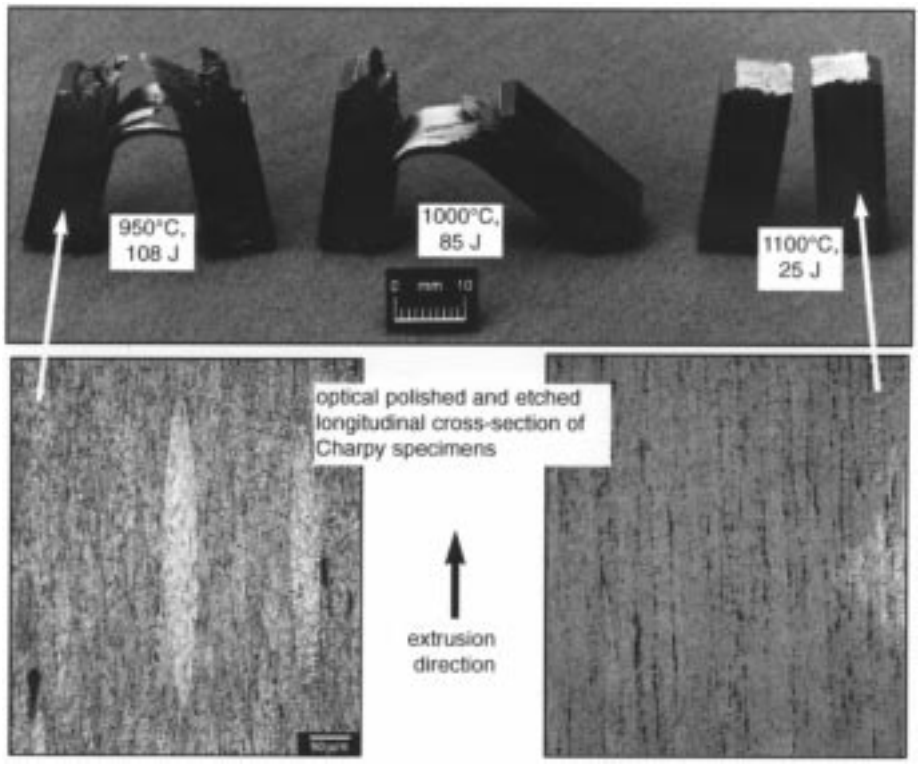

Fig. 14. Fracture of Charpy impact specimens of P/M FeAl consolidated by hot-extrusion at the different temperatures indicated, showing the more ductile fracture associated with the fine-grained and longitudinally elongated remnant prior particle structure found parallel to the extrusion direction [64].

room temperature. The powder products possess mechanical properties comparable to or, in some cases, better than ingot products. Recently, Hajaligol et al. [71] have demonstrated that strips of FeAl aluminides can be commercially produced by an innovative method. Alloy powder together with binder agents were compacted by roll compaction, followed by sintering, heavy cold rolling, and annealing to produce fine and equiaxed grains with close to full density. Mechanical tests indicate that FeAl alloy strips made by this low-cost process have excellent properties at room and elevated temperatures.

The exothermic reaction between Fe and Al has been utilized in both melting and powder consolidation. Using the heat released by the exothermic reaction, Deevi and Sikka [64] have developed the ExoMelt™ process, which substantially shortens melt times, saves energy required for melting, and reduces processing cost. Joslin et al. [72,73] studied the effects of powder particle size, alloy composition, and reaction atmosphere on reaction synthesis of Fe_3Al–FeAl alloys. The reaction took place in both air and vacuum; however, significant amounts of porosity were generated in synthesized products. Further studies are required to reduce porosity and improve the mechanical properties of reaction-synthesized FeAl product.

Iron aluminides are thermodynamically compatible in contact with many ceramics. They are therefore a suitable matrix for a wide variety of composites such as FeAl/WC, FeAl/TiC, FeAl/TiB_2, and FeAl/ZrB_2 [74]. Composites with ceramic volume fractions up to about 60% can be fabricated by liquid phase sintering of a mixture of iron aluminide and ceramic powders at about 1720 K in vacuum. Once the iron aluminide starts to melt, it wets the ceramic particles, porosity is eliminated by capillary action, and a dense composite results. The mechanical strength of the composites depends on the type of ceramic, on the ceramic volume fraction, and on the size of the ceramic particles. For Fe-40 at.% Al containing 60 vol.% WC with a particle size of 5–10 μm, room temperature flexure strengths approaching 1800 MPa and fracture toughness on the order of 20 MPa $m^{1/2}$ have been observed [75].

In the case of WC/Co hard metals, fully dense composites with very high WC volume fractions (90 vol.% and above) can be achieved by liquid phase sintering of mixtures of WC and Co powders. In iron aluminide composites containing more than 60 vol.% of ceramic particles, on the other hand, conventional liquid phase sintering results in substantial porosity as illustrated in Fig. 15a. One important reason for the high porosity is the low solubility of carbides and borides in liquid iron aluminide. While the solubility

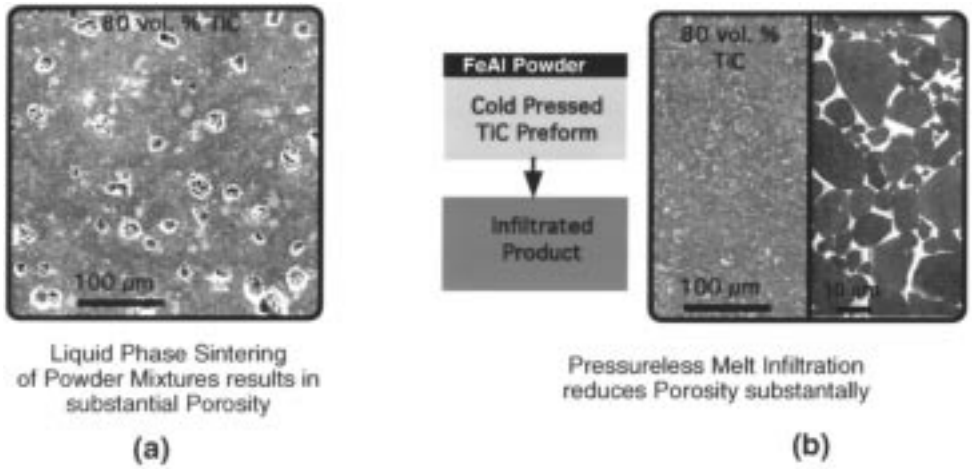

Fig. 15. Processing of Fe-40 at.% Al/80 vol.% TiC compositions by (a) liquid phase sintering of a mixture of FeAl and TiC powders and (b) pressureless melt infiltration of TiC preforms by liquid FeAl [77].

of WC in liquid Co is 24 mol.% at 1500°C [76], the solubilities of carbides and borides in liquid Fe-40 at.% are typically less than 2%. Another reason is that iron aluminide powders tend to form aluminum oxide which is not wetted by liquid iron aluminide. Pressureless melt infiltration provides a convenient solution to these difficulties [77–79]. For example, iron aluminide pieces or powder are put on top of a cold-pressed TiC coupon, which is then heated up in vacuum. As the temperature increases, the TiC undergoes initial-stage sintering. Once the temperature is high enough to melt the iron aluminide, the iron aluminide infiltrates into the remaining porosity in the TiC preform. The melt infiltration process and resulting microstructures are shown in Fig. 15b. Fully dense composites containing 80 vol.% TiC can be fabricated in this manner. Their mechanical properties are superior to those of their conventionally liquid phase sintered counterparts.

As compared to WC/Co, iron aluminide composites are of interest because of low raw material costs, low toxicity, the absence of ferromagnetism, and relatively good oxidation and corrosion resistance [79]. As will be shown below, they are also model systems for basic research aimed at a better understanding of the deformation of iron aluminides. Unless iron aluminides fracture along grain boundaries, they fail by cleavage. In analogy to earlier work by Stroh as well as Cottrell et al. [80] suggested that the cleavage cracks in iron aluminides are nucleated by pile-ups of dislocations against sessile dislocation reaction products. The pile-ups need to have a minimum length in order to generate the stresses needed for crack nucleation. If an iron aluminide ligament in a composite happens to be too thin to accommodate sufficiently long dislocation pile-ups, cleavage cracks cannot be nucleated. This is illustrated in Fig. 16, in which the thinner of the two ligaments fractures in a ductile manner. Assuming the ideal fracture strength to be 1/10 of the elastic modulus E, the critical pile-up length L is given by:

$$L = [b/(5\pi)](E/\sigma)^2,$$

where b is the Burgers vector and σ the tensile stress acting on the ligament. With $E = 180$ GPa, $b = 0.25$ nm, and a ligament fracture stress of $\sigma = 500$ MPa, L is found to be on the order of 2 μm. Consequently,

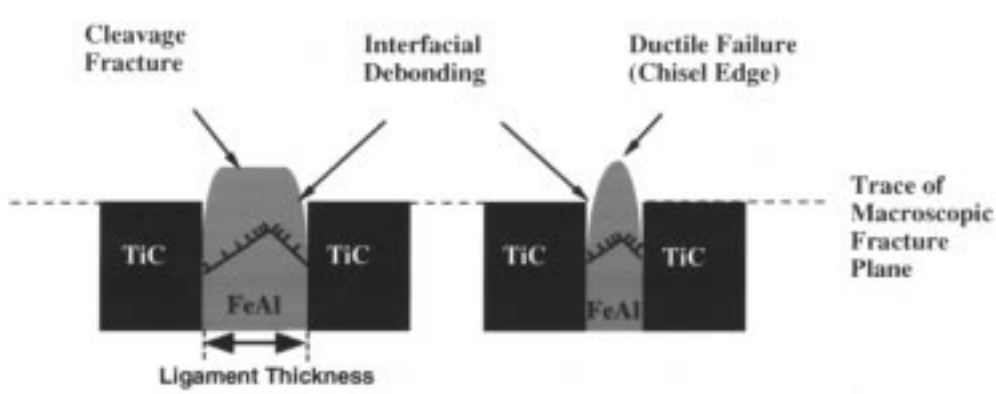

Fig. 16. Schematic of dislocation pile-ups in the FeAl ligaments in Fe-Al composites illustrating the ductile-brittle transition size [81].

ligaments with thicknesses below this size are predicted to fracture in a ductile manner, while the others tend to cleave [81]. The representative micrographs and the statistical distribution of ductile ligaments shown in Fig. 17 are consistent with the calculated value for the critical ligament thickness. It is not clear at the present time to what extent the observed ductile-brittle size transition influences the fracture toughness of iron aluminide composites. There is however tentative evidence that humidity-induced embrittlement is reduced in iron aluminide composites with sufficiently thin iron aluminide ligaments [82]. One probable reason is that these thin ligaments fracture predominantly in a ductile manner and are therefore not likely to be sensitive to humidity-induced embrittlement. Further alloy design of iron aluminides should therefore take the ductile-brittle size transition into account.

FeAl alloys based on Fe-(36–40)Al-0.2Mo-0.05Zr-0.1C-0.01B possess attractive properties for structural applications in hostile environments at elevated temperatures [61–65]. In comparison with Fe_3Al alloys, the FeAl alloys developed have better oxidation and corrosion resistance and relatively lower material density. The unique combination of the excellent resistance to sulfidizing, carburizing, and oxidizing environments at temperatures to 1200°C coupled with low material density and good mechanical properties at temperatures to 800°C has sparked industrial interest in the FeAl alloys and composites for a number of applications:

1. components for coal energy conversion systems (gas–metal filters, cladding for boilers and heat exchangers, etc.),
2. heating elements for various industrial systems,
3. structural components for industrial systems operated in carburizing environments,
4. various food-industry parts (containing no hazardous materials such as Ni and Cr in stainless steels),
5. die-and-tool components,
6. automotive parts: piston valves and rings, exhaust manifolds, catalytic converter substrates, etc.,
7. rails for walking-beam furnaces, and
8. coating materials for improving corrosion resistance.

At present, industries are at various stages of development in the use of FeAl alloys for these applications. A detailed description of the technology developments is given in recent papers by Sikka and Deevi [63,67,71,83].

6. Future research and development

In spite of the current effort on FeAl alloys, a number of areas have been identified for future research and development:

1. vacancy/dislocation interaction at ambient and elevated temperatures,
2. study of vacancy clusters using positron annihilation,
3. hydrogen solubility limit and diffusivity,
4. dislocation–dislocation interaction and slip mode at elevated temperatures,
5. solute site occupation and solute hardening,
6. effect of minor elements on weldability and hot/cold cracking,
7. innovative processing and reduction of manufacturing cost, and
8. generation of data base from large heats.

Acknowledgements

This research was sponsored by the Division of

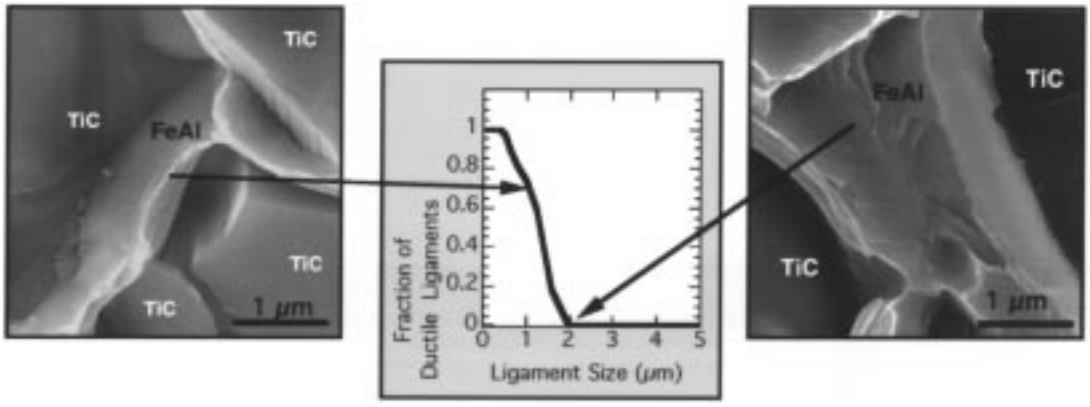

Fig. 17. SEM micrographs illustrating ductile failure for thin iron aluminide ligaments, cleavage fracture for thick ligaments, and the measured size distribution of ductile ligaments [81].

Materials Sciences and the Assistant Secretary for Energy Efficiency and Renewable Energy, Office of Industrial Technologies, Advanced Materials (AIM) Program, US Department of Energy under contract DE-AC05-96OR22464 with Lockheed Martin Energy Research Corp.

References

[1] High-Temperature Ordered Intermetallic Alloys I to VII, MRS Symp. Proc. volumes 39, 81, 133, 213, 268, 364, and 460, MRS, Pittsburgh, PA, 1985–1997.
[2] High Temperature Aluminides and Intermetallics, Mater. Sci. Eng. A152/153, A192/193, and A239/240, 1992–1997.
[3] Structural Intermetallics 1993 and 1997, TMS, Warrendale, PA, 1993 and 1997.
[4] Deformation and Fracture of Ordered Intermetallic Materials, I, II, and III, TMS, Warrendale, PA, 1993–1996.
[5] J.H. Schneibel, M.A. Crimp (Eds.), Processing, Properties, and Applications of Iron Aluminides, TMS, Warrendale, PA, 1994.
[6] S.C. Deevi, V.K. Sikka, P.J. Maziasz, R.W. Cahn (Eds.), International Symposium on Nickel and Iron Aluminides: Processing, Properties, and Applications, ASM, Materials Park, OH, 1997.
[7] S.C. Deevi, D.G. Morris, J.H. Schneibel, V.K. Sikka (Eds.), International Symposium on Iron Aluminides: Alloy Design, Processing, Properties, and Applications, ASM, Materials Park, OH, 1998 (in press).
[8] N.S. Stoloff, Iron aluminides: present status and future prospects, in: S.C. Deevi, D.G. Morris, J.H. Schneibel, V.K. Sikka (Eds.), International Symposium on Iron Aluminides: Alloy Design, Processing, Properties, and Applications, ASM, Materials Park, OH, 1998 (in press).
[9] C.T. Liu, E.H. Lee, C.G. McKamey, Scripta Metall. 23 (1989) 875.
[10] C.T. Liu, E.P. George, Scripta Metall. Mater. 24 (1990) 1285.
[11] C.T. Liu, E.P. George, Mater. Res. Soc. Symp. Proc. 213 (1991) 527.
[12] C.T. Liu, C.L. Fu, E.P. George, G.S. Painter, ISIJ 31 (1991) 1192.
[13] D.J. Gaydosh, M.V. Nathal, Scripta Metall. Mater. 24 (1990) 1281.
[14] W.J. Chia, Y.W. Chung, Intermetallics 3 (1995) 505.
[15] N.R. Gleason, C.A. Gerken, D.R. Strongin, Appl. Surf. Sci. 72 (1993) 215.
[16] N.S. Stoloff, C.T. Liu, Intermetallics 2 (1994) 75–87.
[17] J.W. Cohron, Y. Lin, R.H. Zee, E.P. George, Acta Mater. (1998) submitted.
[18] I. Baker, O. Klein, C. Nelson, E.P. George, Scripta Metall. 30 (1994) 863.
[19] R.J. Lynch, K.A. Gee, L.A. Heldt, Scripta Metall. 7 (1994) 945–950.
[20] M.V. Nathal, C.T. Liu, Intermetallics 3 (1995) 77.
[21] E.P. George, C.T. Liu, in: M.V. Nathal, et al. (Eds.), Structural Intermetallics 1997, TMS, Warrendale, PA, 1997, pp. 693–702.
[22] P. Nagpal, I. Baker, Scripta Metall. 25 (1991) 2577.
[23] D.B. Kasul, L.A. Heldt, Metall. Trans. A 25A (1994) 1285–1290.
[24] L.M. Pike, C.T. Liu, Scr. Mater. 38 (1998) 1475–1480.
[25] D.J. Gaydosh, S.L. Draper, R.D. Noebe, M.V. Nathal, Mater. Scr. Eng. A150 (1992) 7–20.
[26] P. Specht, M. Brede, P. Neumann, MRS Symp. Proc. 364 (1995) 207.
[27] C.L. Fu, G.S. Painter, J. Mater. Res. 6 (1991) 719.
[28] J.C.M. Li, C.T. Liu, Scripta Metall. 27 (1992) 1701.
[29] P.R. Munroe, I. Baker, Acta Metall. 39 (1991) 1011.
[30] M.A. Crimp, K.M. Vedula, Mater. Sci. Eng. 78 (1986) 193.
[31] M.A. Crimp, K.M. Vedula, D.J. Gaydosh, Mater. Res. Soc. Symp. Proc. 81 (1987) 499.
[32] E.P. George, C.T. Liu, D.P. Pope, Acta Mater. 44 (1996) 1757.
[33] J.W. Cohron, E.P. George, L. Heatherly, C.T. Liu, R.H. Zee, Acta Mater. 45 (1997) 2801.
[34] C.T. Liu, C.L. White, J.A. Horton, Acta Metall. 33 (1985) 213.
[35] Y.A. Chang, L.M. Pike, C.T. Liu, A.R. Bilbrey, D.S. Stone, Intermetallics 1 (1993) 107.
[36] H. Xiao, I. Baker, Scripta Metall. Mater. 28 (1993) 1411.
[37] H. Xiao, I. Baker, Acta Metall. 43 (1995) 391–396.
[38] Y. Yang, I. Baker, E.P. George, Mater. Charact. (1998) submitted.
[39] J.H. Westbrook, J. Electrochem. Soc. 103 (1956) 54.
[40] P. Nagpal, I. Baker, Metall. Trans. 21A (1990) 2281.
[41] J.P. Neumann, Y.A. Chang, C.M. Lee, Acta Metall. 24 (1976) 593.
[42] Y.A. Chang, J.P. Neumann, in: W.L. Worrell, G. Rosenbatt (Eds.), Prog. Solid State Chem. 14 (1982) 221.
[43] I. Baker, Mater. Sci. Eng. A192/193 (1995) 1–13.
[44] J.H. Schneibel, Strengthening of iron aluminides by vacancies and/or nickel, in: S.C. Deevi, D.G. Morris, J.H. Schneibel, V.K. Sikka (Eds.), International Symposium on Iron Aluminides: Alloy Design, Processing, Properties, and Applications, ASM, Materials Park, OH, 1998 (in press).
[45] K.M. Chang, Metall. Trans. 21A (1990) 3027.
[46] J.T. Guo, O. Jin, W.M. Yin, T.M. Wang, Scripta Metall. Mater. 29 (1993) 783.
[47] K. Yoshimi, S. Hanada, in: R. Darolia, J.J. Lewandowski, C.T. Liu, P.L. Martin, D.B. Miracle, M.V. Nathal (Eds.), Structural Intermetallics, TMS, Warrendale, PA, 1993, p. 475.
[48] R. Carleton, E.P. George, R.H. Zee, Intermetallics 3 (1995) 433.
[49] E.P. George, I. Baker, Phil. Mag. A 77 (1998) 737.
[50] E.P. George, I. Baker, Intermetallics (1998) in press.
[51] R. Würschum, C. Grupp, H.-E. Schaefer, Phys. Rev. Lett. 75 (1995) 97.
[52] X. Li, I. Baker, Scripta Metall. Mater. 34 (1996) 1219.
[53] E.P. George, R. Carleton, J.W. Cohron, R.H. Zee, (1995) unpublished research.
[54] H.-E. Schaefer, B. Damson, M. Weller, E. Arzt, E.P. George, Phys. Stat. Sol. (A) 160 (1997) 531.
[55] C.G. McKamey, J.H. DeVan, P.F. Tortorelli, V.K. Sikka, J. Mater. Res. 6 (1991) 1779–1805.
[56] V.K. Sikka, S. Viswanathan, C.G. McKamey, in: R. Darolia, J.J. Lewandowski, C.T. Liu, P.L. Martin, D.B. Miracle, M.V. Nathal (Eds.), Structural Intermetallics, TMS, Warrendale, PA, 1993, pp. 483–491.
[57] D.H. Sastry, R.S. Sundar, in: S.C. Deevi, V.K. Sikka, P.J. Maziasz, R.W. Cahn (Eds.), Proceedings of the International Symposium on Nickel and Iron Aluminides: Processing, Properties and Applications, ASM-International, Materials Park, OH, 1997, pp. 123–144.
[58] D. Pocci, O. Tassa, C. Testani, in: J.H. Schneibel, M.A. Crimp (Eds.), Processing, Properties and Applications of Iron Aluminides, TMS, Warrendale, PA, 1994, pp. 19–30.
[59] D.G. Morris, in: S.C. Deevi, V.K. Sikka, P.J. Maziasz, R.W. Cahn (Eds.), Proceedings of the International Symposium on Nickel and Iron Aluminides: Processing, Properties and Applications, ASM-International, Materials Park, OH, 1997, pp. 73–94.
[60] C.T. Liu, V.K. Sikka, C.G. McKamey, Alloy Development of FeAl Aluminide Alloys For Structural Use in Corrosive Envi-

ronments, Oak Ridge National Laboratory Report, ORNL/TM-12199, 1993.
[61] P.F. Tortorelli, P.S. Bishop, Influence of Compositional Modifications on the Corrosion of Iron Aluminides by Molten Nitrate Salts, Oak Ridge National Laboratory Report, ORNL/TM-11598, 1991.
[62] P.J. Maziasz, C.T. Liu, G.M. Goodwin, in: K. Natesan, P. Ganesan, G. Lia (Eds.), Heat Resistant Materials II, ASM-International, Materials Park, OH, 1995, pp. 555–556.
[63] P.J. Maziasz, G.M. Goodwin, D.J. Alexander, S. Viswanathan, in: S.C. Deevi, V.K. Sikka, P.J. Maziasz, R.W. Cahn (Eds.), Proceedings of the International Symposium on Nickel and Iron Aluminides: Processing, Properties and Applications, ASM-International, Materials Park, OH, 1997, pp. 157–176.
[64] S.C. Deevi, V.K. Sikka, Intermetallics 4 (1996) 357–375.
[65] P.J. Maziasz, D.J. Alexander, J.L. Wright, Intermetallics 5 (1997) 547–562.
[66] D.J. Alexander, P.J. Maziasz, J.L. Wright, Processing and alloying effects on tensile and impact properties of FeAl alloys, in: S.C. Deevi, D.G. Morris, J.H. Schneibel, V.K. Sikka (Eds.), International Symposium on Iron Aluminides: Alloy Design, Processing, Properties, and Applications, ASM, Materials Park, OH, 1998 (in press).
[67] P.J. Maziasz, G.M. Goodwin, C.T. Liu, S.A. David, Scripta Metall. Mater. 24 (1990) 1285–1290.
[68] S.C. Deevi, V.K. Sikka, C.T. Liu, Prog. Mater. Sci. 42 (1997) 177–192.
[69] S.C. Deevi, V.K. Sikka, in: S.C. Deevi, V.K. Sikka, P.J. Maziasz, R.W. Cahn (Eds.), International Symposium on Nickel and Iron Aluminides: Processing, Properties, and Applications, ASM, Materials Park, OH, 1997, pp. 283–300.
[70] K.G. Shaw, J.H. Reinshagen, in: S.C. Deevi, V.K. Sikka, P.J. Maziasz, R.W. Cahn (Eds.), International Symposium on Nickel and Iron Aluminides: Processing, Properties, and Applications, ASM, Materials Park, OH, 1997, pp. 301–312.
[71] M.R. Hajaligol, S.C. Deevi, V.K. Sikka, C.R. Scorey, in: S.C. Deevi, D.G. Morris, J.H. Schneibel, V.K. Sikka (Eds.), International Symposium on Iron Aluminides: Alloy Design, Processing, Properties, and Applications, ASM, Materials Park, OH, 1998 (in press).
[72] D.L. Joslin, D.S. Easton, C.T. Liu, S.S. Babu, S.A. David, Intermetallics 3 (1995) 476–481.
[73] D.L. Joslin, D.S. Easton, C.T. Liu, S.A. David, Mater. Sci. Eng. A192/193 (1995) 544–548.
[74] J.H. Schneibel, C.A. Carmichael, E.D. Specht, R. Subramanian, Intermetallics 5 (1997) 61.
[75] J.H. Schneibel, R. Subramanian, K.B. Alexander, P.F. Becher, S.C. Deevi, et al. (Eds.), International Symposium on Nickel and Iron Aluminides: Processing, Properties, and Applications, ASM, Materials Park, OH, 1997, p. 329.
[76] A. Fernandez Guillermet, Metall. Trans. 20A (1989) 935.
[77] J.H. Schneibel, R. Subramanian, in Advances in Powder Metallurgy and Particulate Materials — 1996, vol. 5, Metal Powder Industries Federation, Princeton, NJ, 1996 16-167–16-175.
[78] R. Subramanian, J.H. Schneibel, K.B. Alexander, K.P. Plucknett, Scr. Mater. 35 (1996) 583.
[79] R. Subramanian, J.H. Schneibel, JOM 49 (1997) 50.
[80] P.R. Munroe, I. Baker, Acta Metall. Mater. 39 (1991) 1011.
[81] R. Subramanian, J.H. Schneibel, Acta Mater (in press).
[82] R. Subramanian, J.H. Schneibel, Mater. Sci. Eng. A239/240 (1997) 633.
[83] V.K. Sikka, in: S.C. Deevi, V.K. Sikka, P.J. Maziasz, R.W. Cahn (Eds.), International Symposium on Nickel and Iron Aluminides: Processing, Properties, and Applications, ASM, Materials Park, OH, 1997, pp. 361–376.